CLIMA 2016 - proceedings of the 12th REHVA World Congress

volume 2

Heiselberg, Per Kvols

Publication date:
2016

Document Version
Publisher's PDF, also known as Version of record

Design of a controller model for a concrete core activation floor having air cavities

M. Sourbron[*1], B. van der Heijde[*1,2], B. Battel[1],

R. Vande Ginste[1], D. Picard[1], L. Helsen[1,2]

[1] *Applied Mechanics and Energy Conversion Section, Dept. of Mechanical Engineering, KU Leuven, Celestijnenlaan 300 box 2421, 3001 Leuven, Belgium*

[2] *EnergyVille, Thor Park, Poort Genk 8310, 3600 Genk, Belgium*

[*]Maarten.Sourbron@kuleuven.be, Bram.vanderHeijde@energyville.be

Abstract

The quest towards low-energy buildings renews interest in Concrete Core Activation (CCA), because its low heating and high cooling temperatures harmonise with low-exergy production systems. However, CCA is characterized by a large thermal capacity and thus large time constant, which hampers adequate control. Model based control strategies can overcome this challenge if accurate CCA thermal models are available. But, computation time reduction in applied optimization routines compel simplified models. A sound trade-off between computation speed and accuracy needs thus to be found. In this paper a 1D controller model for an inhomogeneous CCA floor slab with air cavities is constructed. Initial model architecture is based on an available 1D-model for a homogeneous CCA slab and the physical properties of the inhomogeneous CCA slab determine the initial parameters. Firstly, experimental temperature and heat flow data from a full-scale test setup in a controlled environment are used to validate a detailed 3D finite element (FE) model of the CCA floor slab. Secondly, this 3D-FE-model generates multiple response data sets, that are used as training and validation data sets for the parameter identification of the modified 1D controller model. Compared to the 3D-FE-model, the 1D-model predicts steady state heat fluxes with an error smaller than 7.5%, while the time constants of surface heat flux, induced by a step in water supply temperature, are predicted with a maximal error of 6%. The adopted grey-box approach ensures that physics is adequately incorporated in the 1D-model creating model robustness against small dimensional variations.

Keywords – Concrete core activation – TABS – model based control – grey-box model – finite elements – measurements

1. Introduction

Concrete Core Activation (CCA) – also called Thermally Activated Building Systems (TABS) – is a heating and cooling emission system where water tubes are embedded in concrete building floor slabs to ensure thermal comfort in adjacent zones. The large heat exchanging surface allows a low temperature difference with respect to the zone, both for heating and cooling. This on its turn creates opportunities for low exergy production systems, such as heat pumps, direct ground cooling or free cooling using direct outside air. CCA differentiates itself from floor heating systems in the sense that there is

no insulation layer separating the embedded tubes from the constructional part of the floor slab. Moreover, since different types of floor slabs exist, also different types of CCA exist, of which 3 examples are shown in Fig. 1. To reduce weight, hollow cores or air boxes are integrated in the, regarding strength, neutral zone of the slab.

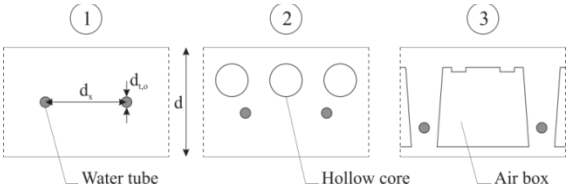

Fig. 1 Comparison between different lay-outs of CCA floor slabs. [1]

However, due to the large thermal mass, the system reacts very slowly to control actions. CCA time constants are in the range of or larger than heating and cooling loads, which seriously hampers an adequate control [2]. The system would benefit from a model-based controller such as not to overheat or undercool the floor, taking into account predictions of future disturbances (e.g. solar irradiation, occupancy) [3]. A Model-based Predictive Controller (MPC) calculates an optimal sequence of control signals to the system, ensuring thermal comfort at the lowest energy cost, taking into account the dynamics of the building and predicted disturbances [4]. The controller model used in the MPC is crucial: it needs to be simple to avoid high computation times, but accurate enough to avoid large discrepancies between the controller model and the actual behavior of the building [5], [6].

The application of MPC in buildings with CCA or floor heating has been studied by several authors ([1], [7]–[15]) where different control formulations are adopted that are however all based on models of the building, CCA and HVAC system. Detailed models calculate 3D or 2D temperature distributions by numerically solving the heat transfer equations [16]–[22], but these are too complex to be used as controller models in an MPC framework.

Fundamental work leading to simplified 1D-modelling of a homogeneous CCA floor slab has been done by Koschenz and Lehmann [23]. They have developed an equivalent resistance network for steady state analysis of TABS, which was extended to a transient RC-model by Weber and Jóhannesson [24] and Weber *et al.* [25]. A shortcoming of their models is that they are valid only in the case of a homogeneous (solid) floor. Sourbron *et al.* [26] suggested an improvement in order to model a floor with cylindrical hollow cores (Fig. 1 middle) based on a 2D FE model and measurements on a scale model of the floor. The influence of the hollow cores is limited to changing the values of the equivalent resistances.

Similarly, a low complexity model has been derived by van der Heijde *et al.* [27], in order to predict the state of charge (SoC) of a homogeneous CCA

slab (Fig. 1 left) with a minimal set of sensors. The authors used grey-box model identification with simulation data from a virtual experiment (3D-FE-model). Here, it was found that a model with two states and the measurement of the surface temperatures and energy leaving/entering the water circuit was sufficient to accurately predict the energy content of the floor.

However, for the current floor lay-out, the air boxes (Fig. 1 right) disturb the layered temperature profile too much (more than the cylindrical hollow cores due to their position in the concrete, size and shape), and the need for a changed model architecture is apparent. This paper studies how the methodology used to develop a grey-box model for SoC determination can be applied to a floor with a slightly different lay-out, namely a floor with air cavities formed with polypropylene boxes having a trapezoidal prism shape.

The **aim of the current paper** is to construct a simple 1D-RC-model, suited to be used in the optimizer of an MPC of this CCA with air boxes. 2D or 3D effects such as floor-to-wall-corners or ventilation exhaust grills are not accounted for. This model should be able to accurately predict heat flows to and from rooms adjacent to the activated building element. The 1D-RC-model architecture is adopted from the existing 1D homogeneous CCA slab model [3]. Initial parameters are derived from the physical properties of the CCA slab with air boxes. An experimental setup generates calibration and validation data for a detailed 3D FE thermal model. This validated 3D-model is used to provide several response data sets that enable the identification of the parameters of the 1D-model.

2. System description

The investigated CCA floor slab has a thickness d (see Fig. 1) of 0.35 m. The air boxes are 0.23 m high and are shaped a trapezoidal prisms (Fig. 1 right). They reduce the floor weight by a factor of 25% to 30% w.r.t. a solid floor and are inversed polypropylene boxes which are inserted in the concrete plate during prefabrication of the floor slab. Furthermore, steel rebar in the lower (12 mm bars) and upper (6 mm bars) concrete layer and welded steel lattice girders are embedded in the floor for constructional reasons. A double polyethylene tube water circuit in the middle part of the slab is considered for the work in this paper. Polypropylene air-boxes, steel rebar, steel lattice girders and polyethylene water tubes all generate inhomogeneity in the CCA floor slab that have to be dealt with while modelling the slab.

3. Methodology

For the floor model, three different layers are considered: a lower layer of reinforced concrete, a middle layer consisting of concrete, steel lattice girders, water tubes and air boxes and an upper layer of again reinforced concrete. Results from the experimental setup are used to tune and validate a detailed 3D-FE-model. Based on this FE-model, calibration data is generated to adapt

the initial values of resistances and capacitances in the simplified 1D-RC-model.

A. Experimental setup

In order to generate experimental data for calibration and validation of the detailed 3D finite elements model, temperature and heat flow measurements are performed on a square CCA floor slab module with sides of 1.2 m. The experimental test floor contains three water circuits at different heights in the slab (one at the bottom, two in the middle) of which only the two middle circuits are considered in this work.

The slab is suspended in the middle of a *heat transfer test room*: an insulated room of 4 x 4 x 3 m^3 of which the walls are covered with radiator panels, constructed according to EN244-2. The radiators allow for complete control of the room temperature. The temperature of the test room walls is set by controlling the water flow through the test room wall panels. The CCA water circuit temperature is controlled by a separate hydraulic circuit of which the set point can be changed independently. A set of 40 T-type thermocouples at representative locations in the CCA slab provides an accurate thermal image of the slab. The calibration of sensors and data-acquisition indicates a measurement error of 0.5°C. White noise is filtered using Matlab's `smooth` function. Furthermore, water entrance and exit temperatures as well as water flow rate are measured for the CCA slab circuit to provide heat flow data from the water circuit to the slab. The hydraulic circuits are fed by pumps that can be switched on or off by the controller. The temperature of both CCA slab and test room circuits is controlled by three way valves and a hot and a cold water storage tank. Step inputs in water supply temperature are applied to the CCA slab circuit. Each measurement starts by equalizing slab and room temperatures, after which the temperature step is applied. Two heating step (15°C to 45°C and 20°C to 30°C) and two cooling step (40°C to 10°C and 25°C to 15°C) experiments are performed. The mean value of the measured water in- and outlet temperatures is used as boundary temperature for the 3D-FE-model. At the upper and lower surface, the measured air and test room wall temperatures serve as boundary temperatures.

B. Finite elements modelling

In a first approach, computational fluid dynamics (CFD) was considered to model the heat transfer in the CCA slab with air boxes. Based on a varying density with temperature according to the Boussinesq equation (1), the natural convection process in the air boxes was represented in addition to the transfer by conduction and radiation:

$$g(\rho - \rho_0) \approx g\beta\rho_0(T - T_0). \quad (1)$$

However, due to the small temperature differences the CFD code could not easily reach convergence. Hence, a different approach was sought in FE

modelling, where, for each inhomogeneity (air boxes, steel rebar, steel lattice girder an water tubes), an equivalent conduction coefficient λ_{eq} is derived.

The steel rebar, steel lattice girders and water tubes are all modelled in detail in the 3D-FE-model. The convection from the water to the pipe wall is calculated according to Gnielinski's [29] correlation for turbulent flow inside a cylinder. Finally, convection and radiation at the slab's surfaces are modelled using standard natural convection and radiation equations.

C. Equivalent conduction coefficient λ_{eq} for the air boxes

To model convection and radiation inside the air boxes, existing correlations for convection and radiation in cavities are used. Convection inside the air cavities is approximated by a correlation of Jakob [30] which describes natural convection in a cuboid cavity with insulated side surfaces as in (2) and (3):

$$Nu = \frac{hL_c}{\lambda} = 0.195 Ra^{1/4}, \quad for\ 4 \cdot 10^4 < Ra < 4 \cdot 10^5\ and\ 0.5 < Pr < 2 \tag{2}$$

$$Ra = \frac{g\beta \Delta T L_c^3}{\nu^2 \alpha} \tag{3}$$

Here, h is the convective heat transfer coefficient, L_c the characteristic length (i.e. the height of the cavity), λ the heat conductivity of the air, g the gravitational acceleration, ΔT the temperature difference between the top and bottom surface, β the compressibility of air, ν the kinematic viscosity and α the thermal diffusivity in air.

In parallel, radiation is modelled by applying the grey body radiative heat exchange equations (ε 0.85 for concrete, 0.97 for polypropylene) and view factors to the air box's geometry. Together with the thermal conductivity of the polypropylene box walls, this leads to a total equivalent thermal conduction coefficient λ_{eq} of the boxes.

Since two parallel water tube circuits are positioned in between the air boxes, leading to approximately equal temperatures at the side walls of the air boxes, convection and radiation between the vertical surfaces are not considered and the air boxes are modelled as a homogeneous material with an equivalent horizontal thermal conductivity $\lambda_{air} = 0.026\ W/mK$.

D. Modification of 3D-FE-model thermal conductivity and capacity values using measurement data

Starting from initial material property values, a sensitivity analysis is performed to determine the influence of material property variations on the resulting temperature distribution in the CCA floor slab. Hence, the material properties that cause temperature variations larger than the measurement error in the experimental setup, are varied in order to find appropriate material property values for the 3D-FE-model (calibration process).

E. 3D-FE-model equivalent conduction coefficient λ_{eq} for concrete with steel rebar, lattice girders and water tubes

Since the measurement setup does not supply information on the heat flows within the CCA floor slab, the 3D-FE-model is used to derive temperature and heat flux data which lead to the determination of equivalent conduction coefficients λ_{eq} for each layer of the CCA floor slab. For the inhomogeneous layers of concrete with steel rebar, with lattice girders and with water tubes, λ_{eq} is determined from $q_{sim} = \frac{\Delta T_{sim}}{R} = \frac{\Delta T_{sim}}{d/\lambda_{eq}}$. These λ_{eq} values are used to determine the thermal resistance values in the 1D-RC-model of the CCA floor slab.

F. 1D-RC-model

The most commonly used simplified model that represents transient heat transfer in concrete slabs is the resistance-capacitance network. Each material layer is represented by a temperature node using a thermal capacity. The nodes are connected by thermal resistances. In reality the capacitance is spread over the entire layer, therefore the model is called the lumped capacity model. The number of capacitances defines the order of the model [1]. The lumped capacity model is typically valid for cases where the thermal conductivity inside a body is much larger than the heat transfer to the surroundings, which is reflected by a small Biot number ($Bi = h_{ext}L/\lambda_{int}$).

However, for the floor under study, *Bi* is rather close to 1 (0.53 and 0.78 for the bottom and top layer, which indicates the presence of a temperature gradient in the floor and contradicts the assumption of lumped capacities. This limits the validity of RC-representations of the layers of the floor. It is argued that the gains in calculation speed outweigh the limited loss in accuracy [23]–[25].

The 1D-RC-model proposed in this paper is built up by three layers: the bottom layer, the top layer and the layer in between, containing the air boxes, see Fig. 2. The upper and lower layers are represented by a capacitance in the middle of the layer, bisecting the resistance of that layer. The middle layer is a parallel network of one branch representing the air boxes and a second branch representing the concrete with water tubes and steel lattice girders.

All **resistances** are derived from the 3D-FE-model (see *3.E*) in which the air boxes have been replaced by homogeneous material with equivalent thermal conductivity . The accuracy of **thermal resistance** values is determined by comparing the steady state heat fluxes of the 1D-model and the 3D model, as these are influenced by the resistances only.

The initial value of the **thermal capacity** of each layer is calculated based on its mass and specific heat of the material. The model only considers the capacity of the concrete and the air box, since the other capacities are negligible.

In Fig. 2, resistances with subscript *t* denote a top layer, *b* a bottom layer. *Y* denotes the result of a star-triangle resistance transformation (see [1]). *p* stands for polypropylene cladding, *a* for air; *wp* denotes the interface between water and concrete. The resistances with *h* refer to convective/radiative surface resistances. The middle layer *m* is divided in a top and bottom part.

The conditions for the 1D-RC-model at the upper and lower slab surface boundaries and at the water boundary inside the tubes are defined by existing correlations from the literature.Convection and radiation from the top and bottom surfaces of the floor are defined by the European standard 15377 [31] to obtain a general 1D-RC-model. This amounts to 11 and 6 W/m^{2}K – convection and radiation combined – for the top, respectively bottom surface in a heating case. For cooling, the values are switched. Convection from the water to the pipe wall is calculated according to Gnielinski's [29] correlation for turbulent flow ($Re \approx 10^4$) inside a cylinder.

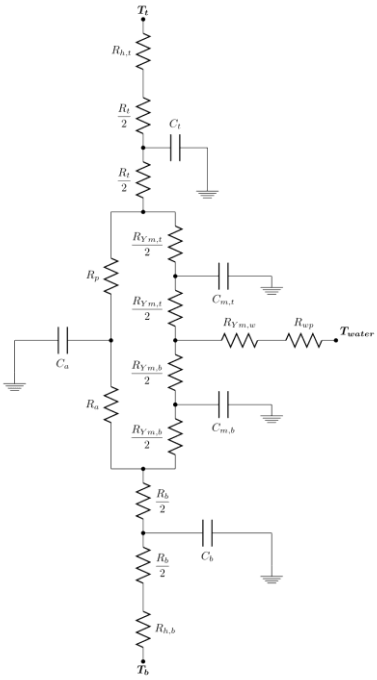

Fig. 2 Schematic of 1D RC-model with water supply in middle layer

4. Results

A. 3D-FE model equivalent conductivity λ_{eq} for the air boxes

When applying the Jakob correlation (3) to the air boxes with an assumed temperature difference of 1 K, a Nusselt number (*Nu*) of 7.27 is found which corresponds to a convective heat transfer coefficient of 0.82 W/m^{2}K between the top and bottom surface of a cavity with a height of 0.23 m. The equivalent conductivity for convection is in this case 0.187 W/mK. Using another correlation proposed by Hollands *et al.* [32], a similar Nusselt number of 7.38 is found.

Applying the radiation heat exchange model and using an assumed temperature difference of 1 K, an equivalent conductivity for radiation of 1.12 W/mK is found. Together with the thermal resistance of the polypropylene box wall (2 mm thickness, $\lambda_{pp} = 0.1$ W/mK) this leads to an equivalent thermal conductivity for the air boxes: $\lambda_{eq} = 1.16$ W/mK, which is about 50% of the conductivity of concrete. The thermal conductance of the air boxes is

0.176 W/m²K (per square meter of floor surface). Radiation is the dominant heat exchange process inside the air boxes.

B. *Calibration of 3D-FE-model thermal conductivity and capacity values using measurement data*

The 3D-FE-model is calibrated and validated using measured temperatures from the experimental setup described in Section 3-A. 97% of the 3D-FE-model data correspond with the measurements, considering a measurement error of ± 0.5 °C. The deviation of the remaining data is due to differences between the 3D-FE-model and the measurement setup. Firstly, difference in the thermal behaviour of the concrete granules (Ø 3 cm) and the cement in between in the real floor causes local temperature gradients, while the thermal properties of the concrete in the 3D-FE-model are assumed uniform. Secondly, the sensor mounting material and cable-wiring are not included in the 3D-FE-model. Finally, the symmetry assumed in the model is not completely satisfied in the real floor. Initial material parameters are taken from technical documentation and literature (see initial values in Table 1).

Table 1 Initial and modified material parameters in the 3D-FE-model

Material	λ [W/mK]	ρ [kg/m³]	c [J/kgK]
Steel	60.50	7850	434
Concrete (initial)	1.80	2300	780
Concrete (modified)	2.30	2000	700
Polyethylene (initial)	0.35	930	2250
Polyethylene (modified)	0.24	930	2250
Polypropylene	0.10	900	1900

Firstly, a sensitivity analysis on the material properties shows that the influence of the properties of steel rebar, steel lattice girders and polypropylene box walls on the temperature profile is smaller than the measurement error of the test setup. Hence, these material properties are not modified.

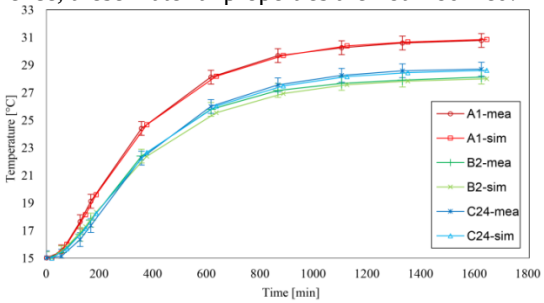

Fig. 3 Measurement *(mea)* data of three sensors and the corresponding 3D-FE-model *(sim)* results

Secondly, in the transient behaviour only the concrete will have a significant influence since it represents 95% of the total thermal capacity. Therefore, the concrete capacity is modified (see Table 1) to match the measurement data (see Fig. 3).

Thirdly, the steady state values of the measurements are used to update the thermal conductivity values of concrete and polyethylene (water tubes). Increasing $\lambda_{concrete}$ and reducing λ_{pe} (see Table 1 for modified values) yields a temperature profile for the 3D-FE-model simulation results, which approximates the measurement values within the measurement accuracy of 0.5°C.

C. 3D-FE-model equivalent conduction coefficient λ_{eq} for concrete with steel rebar, lattice girders and water tubes

Using steady state simulation results of the 3D-FE-model, the equivalent conductivity of the lower and upper layer of concrete with steel rebar is determined. While $\lambda_{concrete} = 2.2$ W/mK in the vertical direction, an equivalent conductivity λ_{eq} of 2.30 for the lower layer, 2.36 W/mK for the upper layer is found for concrete with steel rebar. In the horizontal direction, this is 2.82, resp. 3.10 W/mK.

The influence of the steel lattice girders and water tubes is less important: for the steel lattice girders an equivalent conductivity λ_{eq} of 2.36, 2.33 and 2.32 W/mK is found for the directions vertical, horizontal (parallel to rebar) and horizontal (normal to rebar). The PE-water tubes decrease the thermal conductivity slightly by 2-3%. The equivalent thermal conductivities are used as initial values for the 1D-RC-model of the CCA floor slab.

D. Modification of 1D-RC-model resistance and capacitance values using 3D-FE-model simulation data

As described in the methodology section, the comparison of the 1D and 3D-models' results is used to fine-tune or calibrate the model parameters of the 1D-model by scaling. From the steady state results of the 3D-FE-model, the thermal resistances are calculated as presented in Table 2.

Table 2 Thermal resistance parameters for 1D-model per m^2 of floor surface, in Km^2/W

$R_{Ym,w}$	$R_{Ym,b}$	$R_{Ym,t}$	R_a	R_p	R_b	R_t
0.024	0.034	0.060	20.414	0.046	0.030	0.020

Table 3 Thermal capacitance for 1D-model per m^2 of floor surface, in kJ/Km^2

	C_b	C_{mb}	C_{mt}	C_t	C_a
Original	98	148.4	148.8	70	3.7
Scaled	117.6	178.1	178.1	84	3.7

The maximal error on the steady state heat flux is 7.5% for the 1D-RC-model. This can be explained by the fact that in the 1D-RC-model the upper

and lower layers are homogeneous in temperature, while in the 3D-FE-model, there is a temperature variation due to the presence of the air boxes.

In order to align the transient behaviour of the 1D-RC-model and the 3D-FE-model, the thermal capacity values are increased by 20% (see Table 3); this results in a time constant error of maximal 6% between both models. Fig. 4 presents the comparison between the 3D-FE-model, the original 1D-RC-model and the adapted 1D-RC-model.

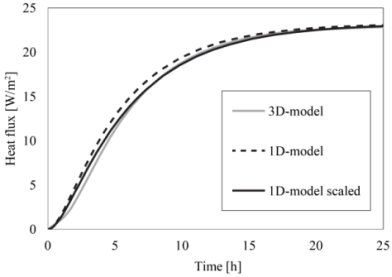

Fig. 4 Comparison of the resulting mean upper surface heat flux from the 3D-model and the original and scaled 1D-models

5. Conclusion

This paper shows how a simple 1D-resistance-capacitance (RC) model can be derived in order to be used for the control of a CCA floor with air cavities. Experiments have been performed on a real setup in a controlled environment, the results of which led to the calibration and validation of a 3D-finite element (FE) model. Using this model, the parameters of a simplified RC model could be derived using a white-box modelling strategy. Special attention was paid to modelling the convective heat transfer in the air cavities, which distincts the current research from previous work. The simulation results from the 1D-RC model have been found to be in accordance with those from the detailed 3D-FE model.

Acknowledgement

The authors would like to thank the company AirDeck Building Concepts for providing a test floor on which the experiments have been conducted. Moreover the authors gratefully acknowledge EFRO/SALK, EU and IWT for funding the research work of Bram van der Heijde, Maarten Sourbron and Damien Picard through the projects EFRO/SALK 936 ‘Towards a Sustainable Energy Supply in Cities’, EU-H20202-GEOTECH ‘Geothermal Technology for Economic Heating and Cooling’ and IWT-VIS-SMART GEOTERM ‘Integration of thermal energy storage and thermal inertia in geothermal concepts for smart heating and cooling of (medium) large buildings’.

References

[1] M. Sourbron, *Dynamic thermal behaviour of buildings with concrete core activation*. Belgium: PhD Thesis, KU Leuven, 2012.

[2] M. Sourbron, R. De Herdt, T. Van Reet, W. Van Passel, M. Baelmans, L. Helsen, R. De Herdt, T. Van Reet, and W. Van Passel, "Efficiently produced heat and cold is squandered by inappropriate control strategies: A case study," *Energy Build.*, vol. 41, no. 10, pp. 1091–1098, 2009.

[3] T. Hilliard, M. Kavgic, and L. Swan, "Model predictive control for commercial buildings: trends and opportunities," *Adv. Build. Energy Res.*, vol. 2549, no. January, pp. 1–19, 2015.

[4] J. M. Maciejowski, *Predictive control: with constraints*. Pearson education, 2002.

[5] A. I. Dounis and C. Caraiscos, "Advanced control systems engineering for energy and comfort management in a building environment—A review," *Renew. Sustain. Energy Rev.*, vol. 13, no. 6–7, pp. 1246–1261, 2009.

[6] P. Bacher and H. Madsen, "Experiments and Data for Building Energy Performance Analysis," Kongens Lyngby, 2010.

[7] M. Sourbron, C. Verhelst, and L. Helsen, "Building models for model predictive control of office buildings with concrete core activation," *J. Build. Perform. Simul.*, vol. 6, no. 3, pp. 175–198, 2013.

[8] T. Y. Chen, "Application of adaptive predictive control to a floor heating system with a large thermal lag," *Energy Build.*, vol. 34, no. 1, pp. 45–51, 2002.

[9] S. H. Cho and M. Zaheer-Uddin, "Predictive control of intermittently operated radiant floor heating systems," *Energy Convers. Manag.*, vol. 44, no. 8, pp. 1333–1342, 2003.

[10] N. T. Gayeski and D. Ph, "Predictive Pre-cooling of Thermo- Active Building Systems with Low- Lift Chillers . Part I : Control Algorithm," *Ashrae*, no. 1999, pp. 1–15, 2011.

[11] H. Karlsson and C.-E. Hagentoft, "Application of model based predictive control for water-based floor heating in low energy residential buildings," *Build. Environ.*, vol. 46, no. 3, pp. 556–569, 2011.

[12] R. W. Wimmer, *Regelung einer Wärmepumpenanlage mit Model Predictive Control*. 2004.

[13] F. Oldewurtel, A. Parisio, C. N. Jones, M. Morari, D. Gyalistras, M. Gwerder, V. Stauch, B. Lehmann, and K. Wirth, "Energy efficient building climate control using Stochastic Model Predictive Control and weather predictions," *Am. Control Conf. (ACC), 2010*, pp. 5100–5105, 2010.

[14] M. Killian, B. Mayer, A. Schirrer, and M. Kozek, "Verteilte kooperative modellprädiktive Temperaturregelung für komplexe Gebäude," *e i Elektrotechnik und Informationstechnik*, vol. 132, no. 8, pp. 474–480, 2015.

[15] J. (Dove) Feng, F. Chuang, F. Borrelli, and F. Bauman, "Model predictive control of radiant slab systems with evaporative cooling sources," *Energy Build.*, vol. 87, pp. 199–210, 2015.

[16] R. A. Meierhans, "Slab cooling and earth coupling," *ASHRAE Trans. Soc. Heat. Refrig. Airconditioning Engin*, vol. 99, no. 2, pp. 511–520, 1993.

[17] K. . Antonopoulos, M. Vrachopoulos, and C. Tzivanidis, "Experimental and theoretical studies of space cooling using ceiling-embedded piping," *Appl. Therm. Eng.*, vol. 17, no. 4, pp. 351–367, Apr. 1997.

[18] M. . Russell and P. . Surendran, "Influence of active heat sinks on fabric thermal storage in building mass," *Appl. Energy*, vol. 70, no. 1, pp. 17–33, Sep. 2001.

[19] B. W. Olesen, M. DE Carli, M. Scarpa, and M. Koschenz, "Dynamic evaluation of the cooling capacity of thermo-active building systems," *ASHRAE Trans.*, pp. 350–357, 2006.

[20] A. Hoh, T. Haase, T. Tschirner, and D. Müller, "A combined thermo-hydraulic approach to simulation of active building components applying Modelica," *Proc. 4th Model. Conf.*, 2005.

[21] J. Babiak, M. Minarova, and B. W. Olesen, “What is the effective thickness of a thermally activated concrete slab?,” in *Proceedings of Clima 2007 WellBeing Indoors*, Helsinki (Finland): FINVAC, 2007.
[22] P. Barton, C. B. Beggs, and P. A. Sleigh, “A theoretical study of the thermal performance of the TermoDeck hollow core slab system,” *Appl. Therm. Eng.*, vol. 22, no. 13, pp. 1485–1499, Sep. 2002.
[23] M. Koschenz and B. Lehmann, *Thermoaktive Bauteilsysteme TABS*. EMPA, 2000.
[24] T. Weber and G. Jóhannesson, “An optimized RC-network for thermally activated building components,” *Build. Environ.*, vol. 40, no. 1, pp. 1–14, Jan. 2005.
[25] T. Weber, G. Jóhannesson, M. Koschenz, B. Lehmann, and T. Baumgartner, “Validation of a FEM-program (frequency-domain) and a simplified RC-model (time-domain) for thermally activated building component systems (TABS) using measurement data,” *Energy Build.*, vol. 37, pp. 707–724, 2005.
[26] M. Sourbron, F. Khaldi, M. Baelmans, and L. Helsen, “Validation of a thermally activated hollow core slab RC-model with measurements and FEM simulations,” *Proc. Symp. Build. Phys.*, vol. 1, no. 1, pp. 3–6, 2008.
[27] B. van der Heijde, E. Carrascal Lecumberri, and L. Helsen, “Experimental Method for the State of Charge Determination of a Thermally Activated Building System (TABS),” in *Proceedings of the Greenstock 13th International Conference on Energy Storage*, 2015.
[28] Airdeck, “Airdeck betonkernactivering,” *Web page*. [Online]. Available: http://www.airdeck.be/nl/?n=152. [Accessed: 16-Dec-2015].
[29] V. Gnielinski, “New equations for heat and mass transfer in turbulent pipe and channel flow (Neue Gleichungen für den Wärme- und den Stoffübergang in turbulent durchströmten Rohren und Kanälen),” *Forsch. im Ingenieurwes.*, vol. 41, no. 1, pp. 8–16, 1975.
[30] M. Jakob, *Heat Transfer*. New York: Wiley, 1949.
[31] E. C. for Standardization, “EN 15377-3 Heating systems in buildings - Design of embedded water based surface heating and cooling systems - Part 3: Optimizing for use of renewable energy sources,” 2007.
[32] K. G. T. Hollands, T. E. Unny, G. D. Raithby, and L. Konicek, “Free Convective Heat Transfer Across Inclined Air Layers,” *J. Heat Transfer*, vol. 98, no. 2, pp. 189–193, May 1976.